Lattice dynamics of La_2NiO_4

L. Pintschovius
Institut für Nukleare Festkörperphysik, Kernforschungszentrum Karlsruhe, Postfach 3640, D-7500 Karlsruhe, Federal Republic of Germany

J. M. Bassat, P. Odier, and F. Gervais
Centre de Recherches sur la Physique des Hautes Températures, Centre National de la Recherche Scientifique, F-45071 Orléans, France

G. Chevrier
Laboratoire Léon Brillouin, Centre d'Etudes Nucléaires de Saclay, F-91191 Gif-sur-Yvette, France

W. Reichardt
Institut für Nukleare Festkörperphysik, Kernforschungszentrum Karlsruhe, Postfach 3640, D-7500 Karlsruhe, Federal Republic of Germany
and Laboratoire Léon Brillouin, Centre d'Etudes Nucléaires de Saclay, F-91191 Gif-sur-Yvette, France

F. Gompf
Institut für Nukleare Festkörperphysik, Kernforschungszentrum Karlsruhe, Postfach 3640, D-7500 Karlsruhe, Federal Republic of Germany
(Received 22 December 1988)

The lattice dynamics of La_2NiO_4, which is isostructural to La_2CuO_4, was investigated by inelastic neutron scattering. All phonon branches were determined in the main symmetry directions [100], [110], and [001]. In addition, the phonon density of states was measured directly on a polycrystalline sample. The results are analyzed on the basis of a rigid-ion model with anisotropic screening of the Coulomb forces to account for the two-dimensional character of the electronic properties. The Coulomb forces were found to lower the frequency of the soft mode at the X point. This mode has the same eigenvector as the soft mode in La_2CuO_4, i.e., it is a tilt mode of the octahedra around a [110] axis. A negative planar breathing deformability of the Ni atom was necessary to reproduce the pronounced anomalies in the branches involving in-plane Ni—O stretching vibrations. A comparison to infrared data yielded very good agreement for modes polarized within the basal plane, whereas a serious disagreement was found for modes polarized along the c axis. A comparison with the data of La_2CuO_4 shows that the lattice dynamics of La_2NiO_4 and La_2CuO_4 are not very different.

I. INTRODUCTION

The knowledge of the vibrational properties of the ceramic high-T_c superconductors is still fragmentary, mainly because of the lack of large single crystals suitable for inelastic-neutron-scattering investigations. As we had grown a large single crystal of La_2NiO_4, which is isostructural to La_2CuO_4, we started on measurements of the phonon dispersion curve of this compound. We hoped that the results for La_2NiO_4 will allow a better understanding of neutron-scattering data obtained on polycrystalline $(La,Sr)_2CuO_4$ samples. Indeed, the vibrational properties of the two systems turned out to be very similar. Unexpectedly, we even observed pronounced anomalies in the phonon dispersion curves of La_2NiO_4 which were predicted by Weber[1] for La_2CuO_4. A short account of the first results was already given in a previous publication.[2] In this paper we report a complete set of phonon dispersion curves for the main symmetry directions and a detailed analysis of these results by model calculations. Furthermore, we present the phonon density of states determined from inelastic-neutron-scattering experiments on a polycrystalline sample. Our results are compared to optical data for La_2NiO_4 and to various data reported for $(La,Sr)_2CuO_4$.

II. EXPERIMENT

The sample was grown by the floating-zone technique. It was of cylindrical shape with a diameter of 7 mm and a length of 25 mm. Its mosaic width was less than 1°. Chemical analysis revealed a deficiency of both La and O, leading to the formula $La_{1.9}NiO_{3.87}$.

The neutron measurements were performed on the 2T triple-axis spectrometer at the ORPHEE reactor at Centre d'Etudes Nucléaires de Saclay. A Cu(111) crystal and a pyrolytic graphite (002) crystal were used as monochromator and analyzer, respectively. Both crystals were

focusing horizontally, which increased the intensity by an order of magnitude, when compared to a conventional setup with the same energy resolution. Of course, the intensity was gained at the expense of resolution in momentum transfer, but this loss is less drastic than often supposed. For transverse phonons focussing effects are less pronounced than in a conventional setup, but still important. For longitudinal phonons focussing effects are often even more favorable for horizontally focussing crystals resulting in a somewhat narrower linewidth. A low final energy of about 14 meV was mostly used also for high-energy excitations yielding a better than normal energy resolution. With horizontally focussing monochromators sample dimensions should not exceed ≈ 1 cm in the horizontal plane. Consequently, 1-cm-wide slits were placed before and after the sample when it was not in an upright position. Examples of phonon groups are given in Fig. 1. Note the short counting times which even for excitations at about 20 THz did not exceed 3 min/point.

The gain in intensity allowed us to speed up the measurements considerably. In total, more than a thousand scans were performed at room temperature, whereby many scans showed more than one phonon line. This wealth of experimental information was extremely useful for the assignment of the observed frequencies. In addition to the room-temperature experiments, selected phonons were investigated also at lower temperatures down to 12 K.

The phonon density of states was determined on a polycrystalline sample prepared in the same way as the single crystals. The neutron measurements were done on the Kernforschungszentrum Karlsruhe time-of-flight spectrometer at the MELUSINE reactor at Centre d'Etudes Nucleaires de Grenoble. Incident neutron energies E_0 of 31.8 and 128 meV were used. With the higher E_0 the whole spectrum could be measured in the neutron-energy-loss mode, but this gave a rather poor resolution for the low-energy part. The fine structure in the low-energy part was obtained from the measurements with small E_0. We note that the spectra were corrected for absorption and multiphonon contributions. The measurements were performed at $T=6$ K, but even at this temperature the multiphonon contributions were appreciable.

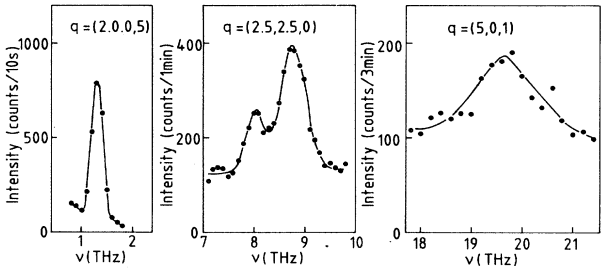

FIG. 1. Examples of phonon groups observed for La_2NiO_4 at room temperature.

III. RESULTS AND ANALYSIS

A. Phonon dispersion curves

La_2NiO_4 has seven atoms per unit cell and hence 21 phonon branches for each direction, which makes it extremely difficult to identify all the branches without the aid of a lattice dynamical model. At the beginning a simple rigid-ion model was set up, and the force constants were tuned to reproduce some ir data[3] and the phonon density of states of La_2CuO_4.[4] Subsequently, this model was refined several times using the accumulating number of experimental phonon frequencies. Both the Born–von Kármán (BvK) force constants and the ionic charges were treated as adjustable parameters. The values of the ionic charges came out considerably smaller than expected from the nominal valency of the atoms, but this is quite usual when fitting rigid-ion models to phonon dispersion curves. Although the models gave a satisfactory overall description of the phonon dispersion curves from the very beginning, the calculated inelastic structure factors were not very reliable. Therefore the assignment of the phonon groups was largely based on the symmetry of the modes. Moreover, measurements were performed in many different Brillouin zones to make the experimental information redundant. The final version of the model yielded a satisfactory description of most of the observed phonon intensities, although some discrepancies remained. The experimental frequencies are depicted in the left-hand part of Fig. 2.

Rather simple models could already explain many features of the dispersion curves, but not all. In particular, there is an LO-TO splitting of $\Delta\nu=2.7$ THz for a Γ-point mode polarized along [001], which is typical of an ionic insulator, whereas—within experimental accuracy—all modes polarized within the basal plane are degenerate, which is typical of a metal. For that reason, the rigid-ion model was modified by an anisotropic screening of the Coulomb forces. For this purpose, we used the following expression for the Coulomb potential

$$V_{ij}(Q,\theta)=\frac{4\pi Z_i Z_j e^2}{Q^2} \times \left\{1-\frac{k_s^2(\theta)e^{-(r_E Q)^2/4}}{Q^2+k_s^2(\theta)}[1+\tfrac{1}{4}(r_E Q)^2]\right\}, \quad (1)$$

where $Z_i e$ are the effective charges of the ions, Q is the momentum transfer, θ is the angle from the [001] direction, and r_E is the relaxation length used in the Ewald summation. $k_s(\theta)$ is the inverse of a screening length. The angular dependence of k_s was assumed to be given by

$$k_s(\theta)=k_{s_0}\sin^2\theta \; . \quad (2)$$

For $\theta=0$ we arrive at the usual expression for the unscreened Coulomb potential

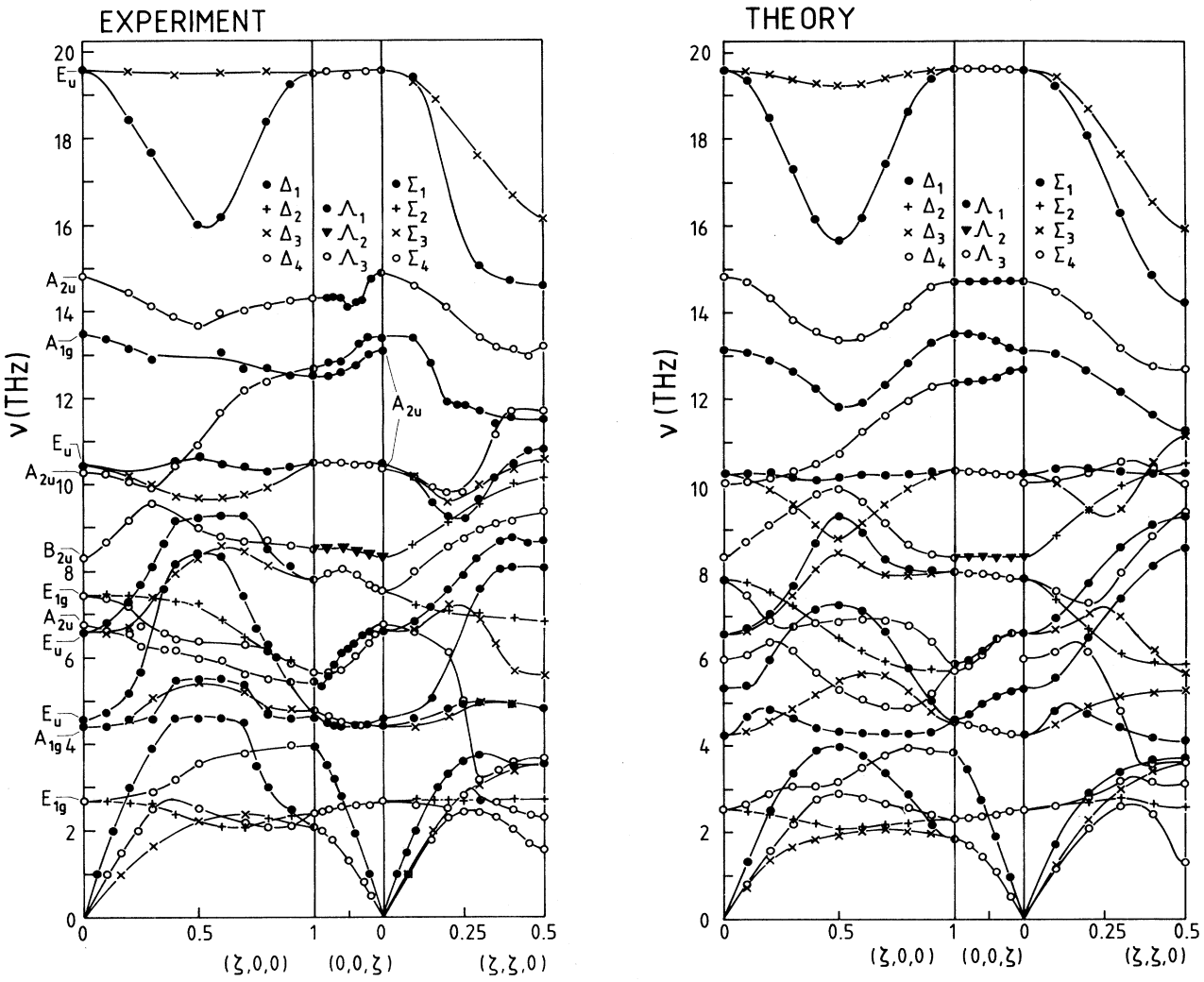

FIG. 2. Experimentally determined (left) and calculated (right) phonon dispersion curves of La_2NiO_4. Lines in the left part of the figure are a guide to the eye only.

$$V_{ij}(Q,0)=\frac{4\pi Z_i Z_j e^2}{Q^2} . \tag{3}$$

For directions in the basal plane ($\theta=90°$) and small Q we have the following behavior:

$$V_{ij}(Q,90°)=4\pi Z_i Z_j e^2\left[\frac{1}{Q^2+k_{s_0}^2}+\frac{1}{32}\frac{k_{s_0}^2 r_E^4 Q^2}{Q^2+k_{s_0}^2}+\cdots\right] . \tag{4}$$

Thus for small Q we get a screened Coulomb potential of the form

$$V_{ij}(r)=\frac{Z_i Z_j e^2}{r}e^{-k_{s_0}r} , \tag{5}$$

the Fourier transform of which is

$$V_{ij}(Q)=\frac{4\pi Z_i Z_j e^2}{Q^2+k_{s_0}^2} . \tag{6}$$

The special form of $V_{ij}(Q)$ in Eq. (1) has the advantage that the Coulomb sum can be calculated without difficulties by the usual method of splitting the sum into two parts, which are summed in real space and reciprocal space, respectively.

Our ansatz to screen the Coulomb forces in the basal plane may be disputed from the fact that La_2NiO_4 is a semiconductor. The carrier concentration which gives rise to the dc conductivity is certainly *too* small to effectively screen the Coulomb forces, at least at wave vectors $q \geq 0.1(2\pi/a)$. Moreover, the screening would be expected to depend strongly on temperature, in contrast to the experimental findings. Perhaps a more realistic way to screen the Coulomb forces in the basal plane would be to introduce a very large polarizability of the

Ni—O_1 bond. This might better correspond to the physics of La_2NiO_4, but our ansatz, too, is in agreement with experiment. Regardless of the way to reproduce the experimental results one can make the following statement: In respect to the lattice dynamics La_2NiO_4 looks like a two-dimensional metal and not like a doped insulator, which means that in spite of strong correlation effects this compound is still on the verge of being a metal.

Even with the inclusion of Coulomb forces, many BvK forces were necessary to obtain a quantitative agreement between model and experiment. Attempts to economize some BvK force constants by introducing a shell model with various shell-core and shell-shell couplings were not successful. However, the introduction of a planar breathing deformability for the Ni ions remarkably improved upon the description of the pronounced dips in the highest longitudinal optic branches in the [100] and [110] directions. In particular, the frequency of the highest Σ_1 mode at the X point, the breathing mode, could be shifted below the frequency of that of the highest Σ_3 mode, the quadrupolar mode. As we pointed out in a previous publication,[2] we consider the dips as caused by a coupling to the electrons. Weber[1] had predicted a breathing instability for La_2CuO_4 by calculations based on the electronic band structure. In order to simulate such an instability of electronic origin we added a 2×2 submatrix $D_{\rm br}$ to the dynamical matrix, which yields a coupling between the x elongation of O_1 at (0.5,0,0) and the y elongation of O_1 at (0,0.5,0):

$$D_{\rm br} = A \begin{bmatrix} \sin^2(\pi q_x) & \sin(\pi q_x)\sin(\pi q_y) \\ \sin(\pi q_x)\sin(\pi q_y) & \sin^2(\pi q_y) \end{bmatrix} . \quad (7)$$

For negative values of A the frequencies of the modes with breathing character are lowered whereas the other frequencies are barely affected. The effect is strongest at the X point and twice as large (in ω^2) as at $\mathbf{q}=(0.5,0,0)$. Figure 3 shows the influence of the breathing term on the calculated frequencies according to our final model. We note that the X point mode at $\nu=11.2$ THz, which is lowered to $\nu=9.3$ THz by the breathing term, has a vibration pattern which is related to that of the breathing mode: In respect to the displacements of the O_1 atoms in the basal plane, it looks like the breathing mode. However, when the O_1 atoms move towards the Ni atoms, the O_2 atoms above and below the plane move away and vice versa. The fact that the low frequency of this mode is in agreement with experiment shows that the breathing term has to be restricted to the in-plane displacements.

The parameters of our final rigid-ion model with anisotropic screening and a planar breathing term which was used to calculate the phonon dispersion curves of Fig. 2 are listed in Table I. Although the model contains 30 Born–von Kármán force constants the agreement between model and experiment is not perfect (root-square-mean deviation $\Delta=0.3$ THz). In the case of $A15$ compounds which likewise have a complex phonon spectrum (24 branches) a clearly better description of the dispersion curves was achieved with the same number of adjustable parameters.[5–7] It is seen that the force constants decrease only slowly with increasing interatomic distances and show strong fluctuations. In particular, the force constants describing the Ni-Ni interaction look highly anomalous. The need for large force constants at longer distances could be traced back to special features in the dispersion curves. Whereas for some features, i.e., the strong depression of modes with breathing character and the large LO-TO splitting of an A_{2u} mode, parameters of clear physical meaning were found, other features could

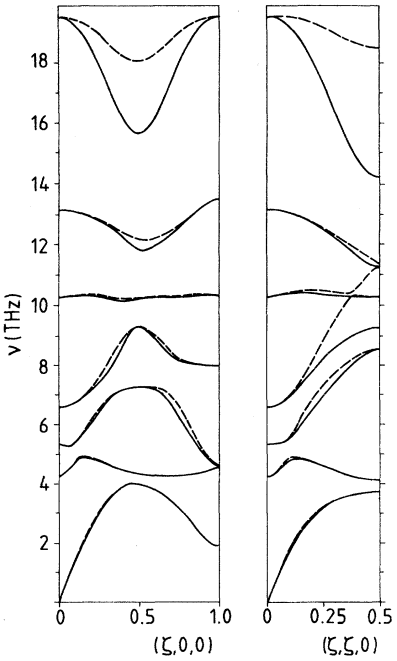

FIG. 3. Calculated phonon dispersion curves with Δ_1 and Σ_1 symmetry with (solid lines) and without (broken lines) a planar breathing deformability.

TABLE I. Parameters of the rigid-ion model with anisotropic screening of the Coulomb forces. Ionic charges La, 1.05; Ni, 0.7; O, −0.7. Breathing force constant $A=-96.6\times10^3$ dyn/cm.

Force constants Pair	Force constants (10^3 dyn/cm) Distance (Å)	Longitudinal	Transverse
Ni-O_1	1.93	172.0	4.0
La-O_2	2.24	70.1	10.4
Ni-O_2	2.47	55.2	9.1
La-O_1	2.52	34.6	−3.7
O_1-O_1	2.73	−0.3	−4.2
La-O_2	2.80	9.4	−2.6
O_1-O_2	2.96	20.8	−1.3
La-Ni	3.18	8.5	−0.8
La-La	3.25	20.3	−0.9
O_2-O_2	3.30	31.8	−2.9
La-La	3.86	15.8	−2.6
Ni-Ni	3.86	−24.0	31.1
O_1-O_1	3.86	−3.6	−4.4
O_2-O_2	3.86	−0.3	−1.1
La-La	4.11	7.1	0
Ni-O_1	4.32	9.3	0

not be described in such a transparent way. As a consequence, we do not attach much significance to the individual force constants at larger distances and do not expect that they can be transferred to models for related compounds.

The soft mode ($\nu=1.6$ THz) at the X point is well reproduced by our model. If branch crossings were not forbidden, the soft mode would not be the endpoint of a transverse acoustic branch, but of a branch starting at $\nu=7.5$ THz. The eigenvector at the X point corresponds to a tilting motion of the octahedra around a [110] axis which is the same as that of the soft mode in La_2CuO_4. Only slight changes of the force constants are necessary to get a zero frequency of this mode. Our analysis showed that the frequency of this mode is lowered by the Coulomb forces. This confirms the idea of Cohen *et al.*[8] that an ionic description of La_2CuO_4 can account for the structural phase transformation.

On cooling to 12 K, the frequency of the soft mode decreased by 15% (see Fig. 4). Thus in our sample the K_2NiF_4 structure was marginally stable, but from Aeppli *et al.*[9] we know that stoichiometric La_2NiO_4 undergoes a tetragonal-to-orthorhombic phase transition at $T\approx240$ K.

Our model analysis shows that the La amplitudes are largest for the flat branches around 2.5 and 4.5 THz, which is not astonishing in view of the heavy mass of the atoms. The largest Ni amplitudes are found in the frequency range between 4 and 11 THz. The frequencies around 19 THz are due to oxygen-nickel stretching vibrations involving O atoms in the basal planes whereas the corresponding out-of-plane modes are centered around 14 THz. Consequently, the force constants for the in-plane and out-of-plane Ni—O bonds differ by a factor of 2. This means that there is a strong anisotropy in the Ni—O bond strength although the anisotropy in bond length is less pronounced than in La_2CuO_4, i.e., 17% instead of 27%. The vibration patterns of all Γ-point modes as well as of some X-point modes are depicted in Fig. 5.

Frequency changes of selected phonons investigated at low temperatures down to 12 K were found to be very small (1–2 %), except for the soft mode at the zone boundary [$\mathbf{q}=(0.5,0.5,0)$].

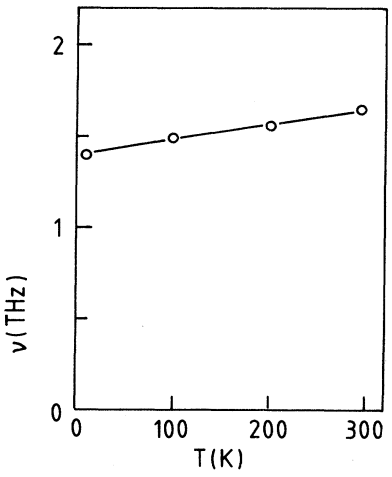

FIG. 4. Temperature dependence of the soft mode at $\mathbf{q}=(0.5,0.5,0)$.

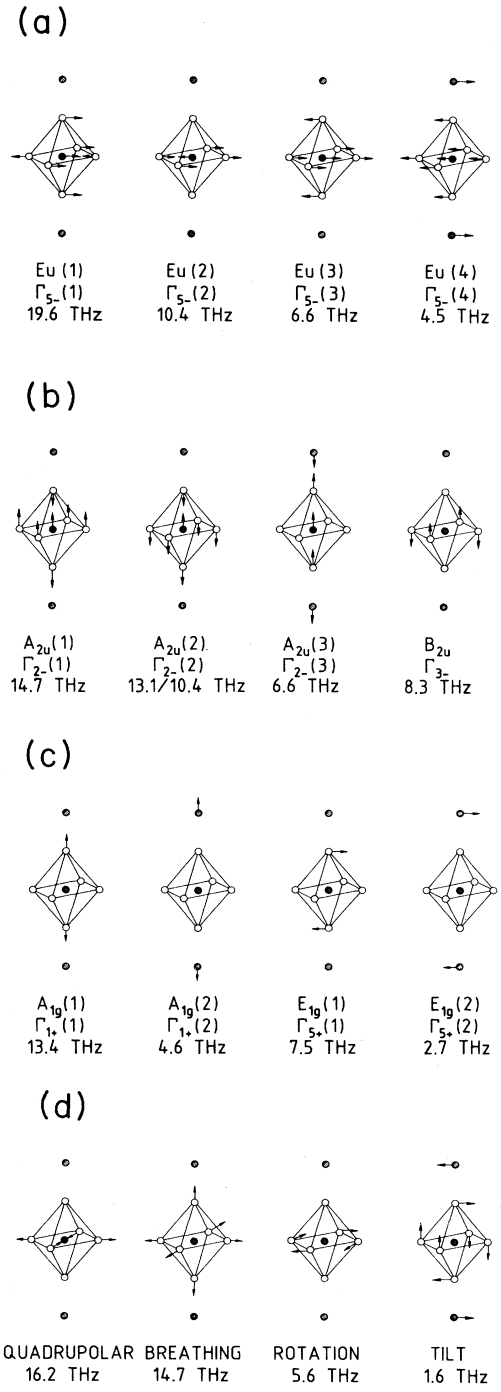

FIG. 5. Eigenvectors of all optical modes at the Γ point and of four modes at the X point. The experimental frequencies are given below. The twofold value for the $A_{2u}(2)$ modes denotes the LO and TO frequencies, respectively.

B. Phonon density of states

Inelastic neutron scattering on polycrystalline samples yields a generalized phonon density of states (PDOS) $G(\nu)$ which differs from the true PDOS $F(\nu)$ by weighting the vibrations of the ith atom with the ratio σ_i/M_i (σ_i is the bound neutron-scattering cross section and M_i is the atomic mass). This factor is largest of O and smallest for La. In Fig. 6 the experimentally determined $G(\nu)$ is compared to the calculated $G(\nu)$. The agreement is not completely satisfactory. Although the calculated phonon dispersion curves in the main symmetry directions do not perfectly reproduce the experimental ones, it appears that these deviations cannot completely explain the differences between the calculated and the observed $G(\nu)$. Small calibration errors of the instruments used may contribute somewhat to the disagreement of peak positions at high frequencies. Further one may suspect that the model yields phonon frequencies for off-symmetry directions less reliable than for the main symmetry lines. Moreover, the model was set up for the stoichiometric compound, whereas the samples are nonstoichiometric. The high-frequency tail of the experimental spectrum is possibly due to a slight contamination with hydrogen. This is suggested by data taken on a first sample which showed by far too much weight in the high-frequency range. A chemical analysis revealed that it contained traces of water corresponding to 50 ppm H. For that reason a second sample was prepared—the results of which are shown here—and great care was taken to avoid any contact with the moisture of the air. Nevertheless, the presence of a few ppm H, which is below the sensitivity of our chemical analysis, cannot be ruled out, which might explain the observed frequencies above 20 THz.

As the generalized phonon density of states is obtained rather directly from the neutron-scattering data, it is the quantity which should be used for comparisons with model calculations (as was done above). However, to evaluate physical quantities as the lattice specific heat, the true phonon density of states $F(\nu)$ is required. There are two ways to get $F(\nu)$ from our results: $F(\nu)$ can be calculated from our model or $F(\nu)$ can be obtained by correcting the experimental $G(\nu)$ with the aid of our model. We think that the latter method gives the more accurate result as the correction factors do not depend sensitively on the model parameters, but are largely determined by the mass ratio of the constituents. Consequently, this method was used to evaluate the phonon spectrum shown in Fig. 7.

C. Magnetic scattering

The interesting magnetic properties of La_2CuO_4 stimulated us to look for magnetic scattering in our sample. However, a search for superlattice peaks at temperatures down to 12 K failed to give any evidence for a magnetic ordering. Meanwhile we know from the work of Aeppli and Buttrey[9] that stoichiometric La_2NiO_4 shows an antiferromagnetic order at $T_N = 70$ K. These authors report a strong reduction of the Néel temperature for a nonstoichiometric sample, and hence it may not be surprising that the rather strong deviation from stoichiometry in our sample suppresses the magnetic ordering completely.

As it is known from Shirane *et al.*[10] that La_2CuO_4 shows strong two-dimensional inelastic magnetic scattering far above the three-dimensional ordering temperature, the absence of a magnetic order in our sample may not exclude the presence of inelastic magnetic scattering intensities. Indeed, at 12 K a weak inelastic signal was found around $\mathbf{q}=(0.5,0.5,0)$ and $\mathbf{q}=(1.5,0.5,0)$. One example is shown in Fig. 8. At 80 K the intensity was greatly reduced, and when further raising the temperature the signal was lost. All observations indicate that the observed intensities are due to dynamic two-dimensional magnetic correlations. These results fit to what is known from previous investigations on $LaNiO_{4+x}$ (Ref. 9) and $LaCuO_{4-x}$ (Ref. 10). The weak intensity of the magnetic signal in our sample prevented a detailed study of this point.

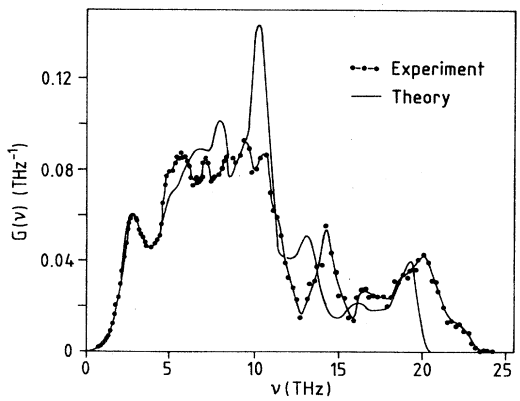

FIG. 6. Experimentally determined and calculated generalized phonon density of states in La_2NiO_4.

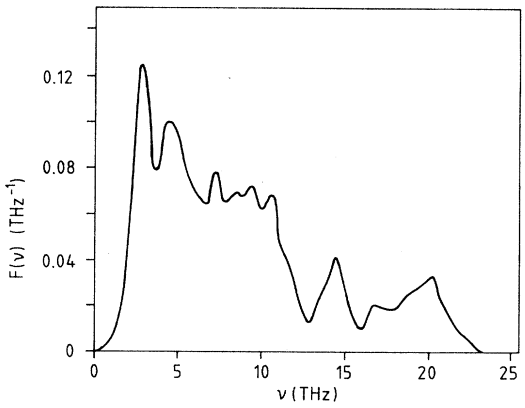

FIG. 7. Phonon density of states of La_2NiO_4. The spectrum was obtained by correcting the experimentally determined generalized phonon density of states with a function calculated with the aid of our lattice-dynamical model.

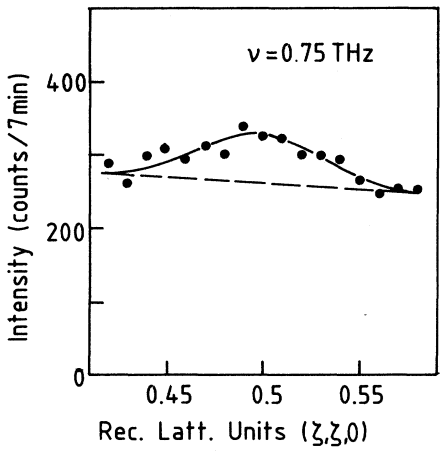

FIG. 8. Example of an inelastic constant-energy scan at $T=12$ K showing dynamic spin correlations. The line is a guide to the eye.

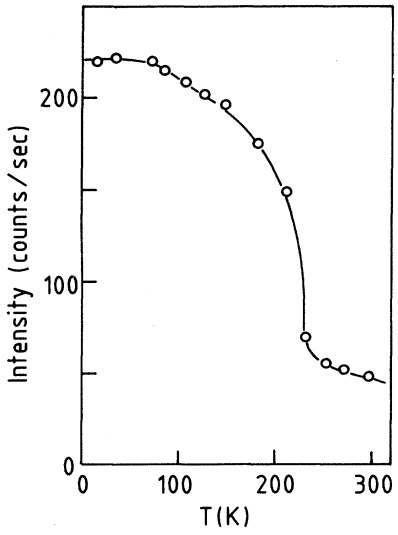

FIG. 9. Peak intensity of the superlattice peak at (1.5,1.5,1.5) vs temperature.

D. Superlattice peaks

As mentioned above, we did not find any superlattice peak of magnetic origin. However, in the course of our search for magnetic peaks we detected some nuclear superlattice peaks. Contributions from higher-order wavelengths were eliminated by the use of very thick filters. Rather strong peaks ($\approx 10^{-3}$ compared to strong fundamental reflections) were found at $(n,0,0)$ with $n=1$, 3, 5, and 7. The intensities did not vary very much neither with Q nor with T. We presume that these peaks are due to an order of the La and/or O vacancies.

A second set of peaks was found at $(h/2,k/2,l/2)$ with h, k, and l odd. The Q dependence of these peaks excludes a magnetic origin but is typical of a nuclear superstructure. The peaks were observable even at room temperature, but their intensity rose sharply when cooling below 230 K (see Fig. 9). Simultaneously, the peaks sharpened, but even at 12 K, they were broader than the experimental resolution when scanned along the [001] direction. From the peak width we conclude that the correlation length did not exceed 40 Å parallel to the c axis. Several attempts were made to find a superstructure giving the observed intensities. The well-known superstructure, which gives rise to the orthorhombic distortion in La_2CuO_4 and stoichiometric La_2NiO_4, has not the right symmetry: It gives rise to superlattice peaks of the type $(h/2,k/2,l)$ with h and k odd and with l even. The soft mode, which is the precursor phenomenon of this superstructure, was found to harden considerably when going from $\mathbf{q}=(0.5,0.5,0)$ to $\mathbf{q}=(0.5,0.5,0.5)$ and hence cannot be related to the superlattice peaks found in our sample. Using a high-resolution setup we looked for a splitting of the (2,2,0) Bragg peak, i.e., for an orthorhombic distortion, but found none. If there is any orthorhombic distortion, it must be smaller than $\Delta a/a \leq 0.1\%$. The superstructure, which was found to give the best agreement between calculated and observed superlattice peak intensities, consists of a slight distortion of the octahedra. In the basal plane, the octahedra are alternately expanded and contracted in both directions. Those octahedra, which are expanded in the basal plane, are shortened along the c axis and vice versa, i.e., the Jahn-Teller-type distortion of the octahedra is modulated. The La atoms follow somewhat the displacement of the O atoms along the c axis and thereby arrange the correlation between different planes. However, this model reproduces the observed intensity pattern only qualitatively. It turned out that only the assumption of a multidomain structure allowed sufficient degrees of freedom for a further refinement of the model. In view of the complexity of the problem it was not pursued any further.

E. Comparison with optical data

Infrared data for La_2NiO_4 are reported by Bassat *et al.*[3] and Gervais *et al.*[11] From the modes polarized in the basal plane, the four E_u modes at $\nu=19.6$, 10.5, 6.6, and 4.4 THz should show up in the infrared (ir) spectrum for the electric field E of the electromagnetic radiation $E \perp \hat{c}$. Three of these modes (19.6, 10.5, and 4.4 THz) are nicely seen at the expected positions.[3] At 80 K an indication is seen also for the mode with $\nu=6.6$ THz.[11] In contrast to the very good agreement between ir and neutron data for the modes polarized in the basal plane, there is complete disagreement for the modes polarized along c. There are 3 A_{2u} modes which should show up in the ir spectrum. According to our analysis, the LO-TO modes have the following frequencies: 14.8-14.8 THz, 13.1-10.4 THz, 6.6-6.6 THz. Due to the finite resolution of the neutron measurements, small LO-TO splittings of the highest and the lowest A_{2u} modes ($\Delta\nu \leq 0.3$ THz) may have been overlooked. The ir data give LO-TO frequencies at $\nu=17.6$-15 THz and $\nu=14.4$-8.2 THz. We found no way to reconcile these data with the neutron results. We tried different assignments of the neutron frequencies, but this removed the discrepancies only partly and

caused serious disagreements between the observed and calculated intensities of the phonon peaks. A special search was undertaken to find an A_{2u} mode at $\nu=17.6$ THz without success. So the disagreement between neutron and ir data remains a puzzle. In view of the similarity of the ir spectra for La_2NiO_4 and La_2CuO_4 (Ref. 11) and of the neutron data as well (see below) an analogous discrepancy has to be expected for La_2CuO_4. Moreover, the Raman data for La_2CuO_4 (Refs. 12 and 13) are likewise anomalous: A prominent mode is observed at $\nu=15.9$ THz (530 cm^{-1}) which could not be assigned to a Raman allowed mode. It remains unclear which feature of these compounds gives rise to their peculiar behavior in light-scattering experiments.

F. Comparison to La_2CuO_4

The fact that La_2NiO_4 and La_2CuO_4 are isostructural with very similar dimensions of the unit cell suggests that the lattice dynamics of the two compounds may be similar. This expectation is confirmed by experiment. In Fig. 10 we show a comparison of the generalized phonon density of states of La_2NiO_4 and doped $LaCuO_4$.[4] The similarity of the spectra is striking. As the spectra of doped and pure La_2CuO_4 differ only little, a comparison between La_2NiO_4 and pure La_2CuO_4 would yield a very similar result as well.

A more detailed comparison has to be based on the phonon dispersion curves. So far published data on the phonon dispersion curves of La_2CuO_4 (Ref. 14) and $(La,Sr)_2CuO_4$ (Ref. 15) cover only a few low-frequency branches. Nevertheless, Böni *et al.*[15] concluded that La_2NiO_4 is not a good reference system for $(La,Sr)_2CuO_4$. This view was based on two arguments: First, they noted that there is no softening of the LA mode in the [111] direction near the zone boundary in $(La,Sr)_2CuO_4$. However, a comparison shows that this branch is not very different for the two compounds (see Fig. 11). If Böni *et al.*[15] consider the slight frequency decrease towards the zone boundary in La_2NiO_4 to be an important feature, they presumably assume that it is caused by an interaction with the highest Σ_1 branch, i.e., strictly speaking by the breathing instability. This interpretation, however, is speculative. It is true that the breathing mode has an anomalously low frequency, but not to such an extent as to make an interaction with the LA mode obvious. According to our analysis, the LA branch is only slightly affected by the breathing deformability (see Fig. 3). Instead, the shape of the LA branch may simply result from an interaction with the flat branch of La vibrations of $\nu\approx4.5$ THz.

The second argument of Böni *et al.*[15] for "significant differences" between the lattice dynamics of La_2NiO_4 and $(La,Sr)_2CuO_4$ was the observation that the lowest phonon mode at the zone boundary in the [110] direction is harder in La_2NiO_4. In this context, we want to emphasize that *both* compounds show a soft mode having the same eigenvector. If this soft mode is marginally stable in our sample of La_2NiO_4, this can hardly be seen as a fundamental difference to $(La,Sr)_2CuO_4$. Given the fact that the frequency of this mode depends on a delicate balance between short range and Coulomb forces, it is not surprising that this frequency depends sensitively on the stoichiometry of the sample. As mentioned in Sec. III A, stoichiometric La_2NiO_4 shows a tetragonal-to-orthorhombic phase transition at $T\approx240$ K,[9] which definitely rules out any fundamental difference.

Recently, a neutron-scattering study on La_2CuO_4 was started aiming at the phonon dispersion in the entire frequency range up to 20 THz.[16] Using first results we have plotted a comparison of the branches with Δ_3 symmetry for La_2CuO_4 and La_2NiO_4 in Fig. 12. As was to be expected from the comparison of the phonon densities of states, the frequencies are strikingly similar but not identical. Only an analysis of the full set of dispersion curves will tell us the origin and the relevance of the differences.

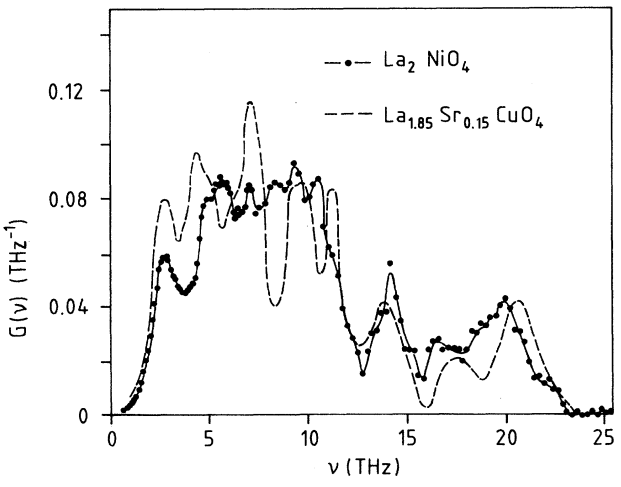

FIG. 10. Comparison of the experimentally determined generalized phonon density of states of La_2NiO_4 and $La_{1.85}Sr_{0.15}CuO_4$ (Ref. 4).

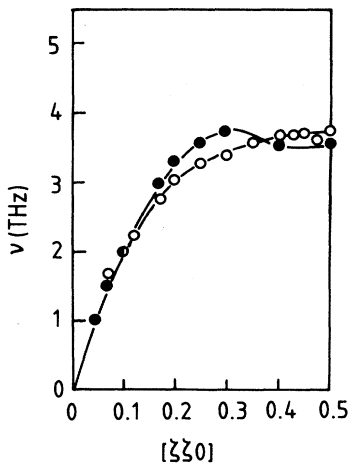

FIG. 11. Comparison of the LA(111) branch in La_2NiO_4 (solid circles) and $(La,Sr)_2CuO_4$ (open circles, Ref. 14).

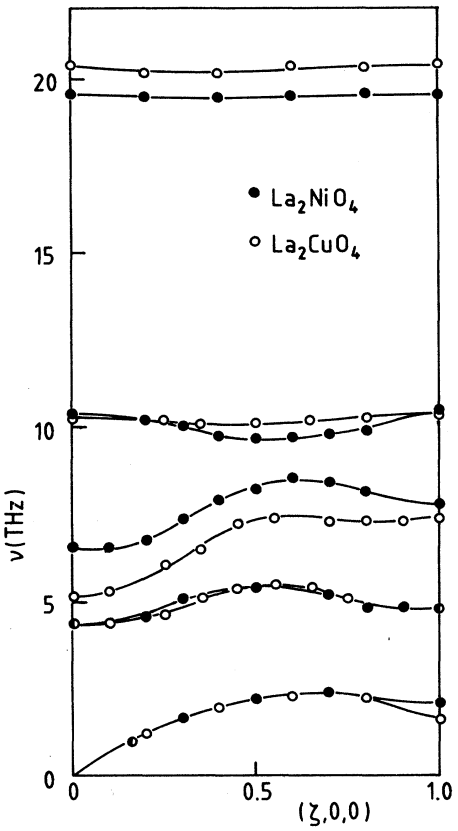

FIG. 12. Comparison of the phonon branches with Δ_3 symmetry for La_2NiO_4 and La_2CuO_4 (Ref. 15).

IV. CONCLUSIONS

We have determined a complete set of phonon dispersion curves of La_2NiO_4 in the main symmetry directions. Model calculations based on these data showed that a complicated force field in necessary to describe all essential features of the dispersion curves. In particular, Coulomb forces are indispensible to describe some branches polarized along the c axis, but these forces have to be screened for the branches polarized in the basal plane, which means that in respect to the lattice dynamics La_2NiO_4 looks like a two-dimensional metal. A planar breathing deformability is necessary to reproduce anomalous features in the high-frequency branches involving in-plane Ni—O stretching vibrations. These anomalies indicate a strong electron-phonon coupling for these modes. We note that this case is analogous to the case of mixed-valent compounds where pronounced phonon anomalies could be well described by a breathing shell model.[17–19] In the mixed-valent compounds, however, the negative breathing deformability applied to the motion of the surrounding atoms in all three directions, whereas in La_2NiO_4 only the in-plane O motions are of importance.

A search for magnetic scattering intensities yielded evidence for two-dimensional dynamic spin correlations, but no static magnetic order was found, presumably because of the nonstoichiometry of the sample. Nuclear superlattice peaks indicate a superstructure at low temperatures which involves a modulation of the distortion of the octahedra.

A comparison of the neutron results to ir data yielded a very good agreement for modes polarized within the basal plane, whereas a serious disagreement was found for modes polarized along the c axis. This discrepancy remains a puzzle.

Comparison of the data for La_2NiO_4 and La_2CuO_4 shows a very close relationship of the lattice dynamics of the two compounds. Therefore La_2NiO_4 seems to be a suitable reference system for investigation at the interaction between electrons and lattice vibrations in $(La,Sr)_2CuO_4$.

ACKNOWLEDGMENTS

Laboratoire Léon Brillouin is Laboratoire commun Commissariat à l'Energie Atomique–Centre National de la Recherche Scientifique (CEA–CNRS).

[1]W. Weber, Phys. Rev. Lett. **58**, 1371 (1987); **58**, 2154(E) (1987).
[2]L. Pintschovius, J. M. Bassat, P. Odier, F. Gervais, B. Hennion, and W. Reichardt, Europhys. Lett. **5**, 247 (1988).
[3]J. M. Bassat, P. Odier, and F. Gervais, Phys. Rev. B **35**, 7126 (1987).
[4]B. Renker, F. Gompf, E. Gering, N. Nücker, D. Ewert, W. Reichardt, and H. Rietschel, Z. Phys. B **67**, 15 (1987).
[5]L. Pintschovius, H. G. Smith, N. Wakabayashi, W. Reichardt, W. Weber, G. W. Webb, and Z. Fisk, Phys. Rev. B **28**, 5866 (1983).
[6]H. G. Smith, N. Wakabayashi, Y. K. Chang, L. Pintschovius, and W. Weber, Phys. Rev. B **31**, 7772 (1985).
[7]L. Pintschovius, M. Takei, and N. Toyota, Phys. Rev. Lett. **54**, 1260 (1985).
[8]R. E. Cohen, W. E. Pickett, L. L. Boyer, and H. Krakauer, Phys. Rev. Lett. **60**, 817 (1988).
[9]G. Aeppli and D. J. Buttrey, Phys. Rev. Lett. **61**, 203 (1985).
[10]G. Shirane, Y. Endoh, R. J. Birgeneau, M. A. Kastner, Y. Midaka, M. Oda, M. Suzuki, and T. Murakami, Phys. Rev. Lett. **59**, 1613 (1987).
[11]F. Gervais, P. Eckegut, J. M. Bassat, and P. Odier, Phys. Rev. B **37**, 9364 (1988).
[12]G. A. Kouruoklis, A. Jayaraman, W. Weber, J. P. Remeika, G. P. Espinosa, A. S. Cooper, and R. G. Maines, Sr., Phys. Rev. B **36**, 7218 (1987).
[13]A. I. Maksimov, O. V. Misachku, I. T. Tartakovsky, V. B. Timofeev, J. P. Remeika, A. S. Cooper, and Z. Fisk, Solid State Commun. **66**, 1077 (1988).
[14]R. J. Birgeneau, C. Y. Chen, D. R. Gabbe, H. P. Jenssen, M. A. Kastner, C. S. Peters, P. J. Pirane, T. Thio, T. R. Thurston, M. L. Tuller, J. D. Axe, P. Böni, and G. Shirane, Phys. Rev. Lett. **59**, 1329 (1987).
[15]P. Böni, J. D. Axe, G. Shirane, R. J. Birgeneau, D. R. Gabbe, H. P. Jenssen, M. A. Kastner, C. J. Peters, P. J. Picone, and

T. R. Thurston, Phys. Rev. B **38**, 185 (1988).
[16]A. Rumyantsev, L. Pintschovius, and W. Reichardt (unpublished).
[17]H. A. Mook, R. M. Nicklow, T. Penny, F. Holtzberg, and M. W. Shafer, Phys. Rev. B **18**, 677 (1978).
[18]H. Bilz, G. Güntherodt, W. Kleppmann, and W. Kress, Phys. Rev. Lett. **43**, 1998 (1979).
[19]A. Severing, W. Reichardt, E. Holland-Moritz, D. Wohlleben, and W. Assmus, Phys. Rev. B **3**, 1773 (1988).